Tubular epithelial cell HMGB1 promotes AKI-CKD transition by sensitizing cycling tubular cells to oxidative stress. A rationale for targeting intracellular HMGB1 during AKI recovery

Zhi Bo Zhao[1*], Julian A. Marschner[1*], Takamasa Iwakura[1], Chenyu Li[1], Manga Motrapu[1], Meisi Kuang[1], Bastian Popper[2], Andreas Linkermann[3], Jan Klocke[4], Philipp Enghard[4], Yoshiharu Muto[5], Benjamin D. Humphreys[5,6], Helena Erlandsson Harris[7], Paola Romagnani[8], Hans-Joachim Anders[1]

1 Nephrologisches Zentrum, Medizinische Klinik und Poliklinik IV, Klinikum der Universität München, LMU München, Germany
2 Biomedical Center, Core Facility Animal Models, LMU München, Germany
3 Division of Nephrology, Department of Internal Medicine 3, University Hospital Carl Gustav Carus at the Technische Universität Dresden, Dresden, Germany
4 Department of Nephrology and Medical Intensive Care, Charité-Universitätsmedizin Berlin, Corporate Member of Freie Universität Berlin and Humboldt-Universität zu Berlin, Germany.
5 Division of Nephrology, Department of Medicine, Washington University in St. Louis, St. Louis, MO, USA
6 Department of Developmental Biology, Washington University in St. Louis, St. Louis, MO, USA
7 Departments of Rheumatology and of Medicine Solna, Center for Molecular Medicine, Karolinska Institutet, Stockholm, Sweden
8 Department of Experimental and Biomedical Sciences "Mario Serio" and Nephrology and Dialysis Unit, Meyer Children's University Hospital, Florence, Italy

Supplementary material

Supplementary table 1: Narcosis, antagonization and analgesia 2
Supplementary table 2: Antibodies and reagents for immunohistochemical and immunofluorescence staining 3
Supplementary table 3: PCR reaction mixtures 4
Supplementary table 4: Primer pairs used for qPCR and genotpying 5
Supplementary table 5: Primary murine tubular cell culture medium composition 5
Supplementary table 6: Reagents, antibodies and kits 6
Supplementary figure 1 7
Supplementary figure 2 8
Supplementary figure 3 9
Supplementary figure 4 10
Supplementary figure 5 11
Supplementary figure 6 12
Supplementary figure 7 13
Supplementary video 1 14
Supplementary video 2 14

Supplementary table 1: Narcosis, antagonization and analgesia

Drug	Concentration [mg/kg BW]	Treatment regime	Cat number	Company
		Narcosis		
Medetomidine	0.5	i.p. injection, once prior to surgery, surgical tolerance verified by toe pinching	07725752	Zoetis
Midazolam	5		4921530	ratiopharm
Fentanyl	0.05		2084366	Janssen-Cilag
		Antagonization		
Atipamezol	5	s.c. injection, once	8-00732	CP-Pharma
Flumazenil	0.1		4470990	Hexal
		Analgesia		
Buprenophin	0.1	i.p. injection, once 30min prior to antagonization, then every 8h for 3 consecutive days	01498870	Bayer Vital
Metamizol-Natrium 1H2O	200	p.o. application, 5min prior to narcosis induction	0731672	Sanofi-Aventis

Supplementary table 2: Antibodies and reagents for immunohistochemical and immunofluorescence staining

Antibody for antigen (rabbit anti-mouse)	Target/ host	Secondary antobidy/ avidin-biotin complex	Dilution/ incubation time	Cat number	Company
		Primary antibodies			
LTL, biotinylated	Mouse	VECTASTAIN	1:250 PBS/ 1h RT	B-1325	Vector
THP	Mouse/ rabbit	Biotinylated goat anti-rabbit IgG/ VECTASTAIN	1:2000 (10% milk)/ over night 4°C	sc-20631	Santa Cruz
Nitrotyrosine	Mouse/ mouse	Biotinylated rat anti-mouse IgG2a/ VECTASTAIN	1:50 (10% milk)/ over night 4°C	NB110-96877	Novus Bio
		Secondary antibodies			
IgG (H+L), biotinylated	Rabbit/ goat	-	1:300 PBS/ 30min RT	ZRB1001	Linaris
IgG2a, biotinylated	Mouse/rat	-	1:300 PBS/ 30min RT	553388	BD Pharming
		Avidin-biotin complex/ substrate			
VECTASTAIN® ABC Kits	-	-	-	PK6100	Vector Laboratories
3,3'-Diamino-benzidine	-	-	-	H54000	Alfa Aesar

Supplementary table 3: PCR reaction mixtures

Reagent	Amount per reaction [µl]	Company	Cat number
Reverse transcriptase PCR			
dNTP Set (25 mM per base)	0.45	Thermo Fisher Scientific	R0186
DTT 0,1 M	1	Thermo Fisher Scientific	18080085
5x First Strand Buffer	4.5	Thermo Fisher Scientific	18080085
Hexanucleotide Mix	0.25	Roche Diagnostics	11277081001
Linear Acrylamide (15 µg/ml)	0.25	Thermo Fisher Scientific	AM9520
RNasin R Ribonuclease Inhibitor	0.5	Promega	N2515
SuperScript TM III Reverse Transcriptase or ddH2O	0.5	Thermo Fisher Scientific	18080085
Quantitative real-time PCR			
BioStab PCR Optimizer	4	Biomol	62508.5
Bovine Serum Albumin PCR grade	0.2	Thermo Fisher Scientific	B14
ddH2O PCR grade	1.2	Invitrogen	10977035
dNTP Set (25 mM per base)	0.15	Thermo Fisher Scientific	R0186
MgCl 2 25mM	2.4	Thermo Fisher Scientific	R0971
Primer forward 10µM	0.6	Metabion international	-
Primer reverse 10µM	0.6	Metabion international	-
SYBR R Green I nucleic acid gel stain	0.04	Sigma-Aldrich Chemie	86205
Taq DNA Polymerase	0.16	New England Biolab	M0273X
10X Taq Buffer without Detergent	2	Thermo Fisher Scientific	B55

Supplementary table 4: Primer pairs used for qPCR and genotpying

Target gene	NCBI key	Forward primer	Reverse primer
Hmgb1	XM_024449341.1	TACTCGGAGAAACTTCAGACCG	TAACGAGCCTTGTCAGCCTT
Rn18s	NR 003278.3	GCAATTATTCCCCATGAACG	AGGGCCTCACTAAACCATCC
Ngal	NM_008491.1	ATGTCACCTCCATCCTGG	GCCACTTGCACATTGTAG

Supplementary table 5: Primary murine tubular cell culture medium composition

Reagent	Company	Cat number	Volume
DMEM + GlutaMAX™	Thermo Fisher Scientific	21885-025	450ml
FBS	Biochrom	S0115	50ml
HEPES Cell culture grade (1M, pH 7.55)	AppliChem GmbH	A3268,9025	12.5ml
Penicillin/ streptomycin	PAN Biotech GmbH	P06-07100	5ml
Hank's Balanced Salt Solution	Thermo Fisher Scientific Inc.	14025-092	5ml
Epidermal growth factor 12.5ug/ml	Genscript	Z02972	1ml
Insulin transferrin-sodium selenite supplement 10mg/ml	Roche Diagnostics GmbH	11074547001	500ul
Hydrocortisone 1.8ug/ml in ethanol	Sigma-Aldrich	H0888	50ul
3,3',5-Triiodo-L-thyronine sodium salt (T3) at 2.4ng/ml in ethanol	Sigma-Aldrich	T5516	5ul
Prostaglandin E1 125ng/ml in ethanol	Sigma-Aldrich	P7527	1.25ul

Supplementary table 6: Reagents, antibodies and kits

Reagent	Company	Cat number
Cytotoxicity Detection Kit (LDH)	Roche Diagnostics	11644793001
CellTiter 96® Non-Radioactive Cell Proliferation Assay	Promega	G4100
Collagenase IV	Sigma-Aldrich	C4-BIOC
Collagenase D	Roche Diagnostics	1108886600
IgG2b	Sigma	MOPC-195
Percoll®	Sigma-Aldrich	P1644
Pre-sepereation filter, 70 µm pore diameter	Miltenyi Biotec	130-095-823
Solubilization/ Stop Solution	Promega	G4101
Breeder Brinsea Octagon 20 Advance	J.Hemel Brutgerät	32150
FITC-labeled sinistrin	MediBeacon	NA
Pure Link RNA Mini Kit	Invitrogen	12183018A
RET-3-ISO Isolated Rectal Probe for Mice	Physitemp Instruments	NA
RNAlater	Ambion,	AM7021
Rodent surgery table (heatable)	Medax	M12511
Suture Ethibond Excel 5-0	Ethicon	EH7260H
Suture Vicryl TM 5-0	Ethicon	V493H
Thermes-USB Temperature Data Acquisition Seven channel unit	Physitemp Instruments	NA
Yasargil Aneurysm Clip	Medicon	58.54.10

Supplementary figure 1

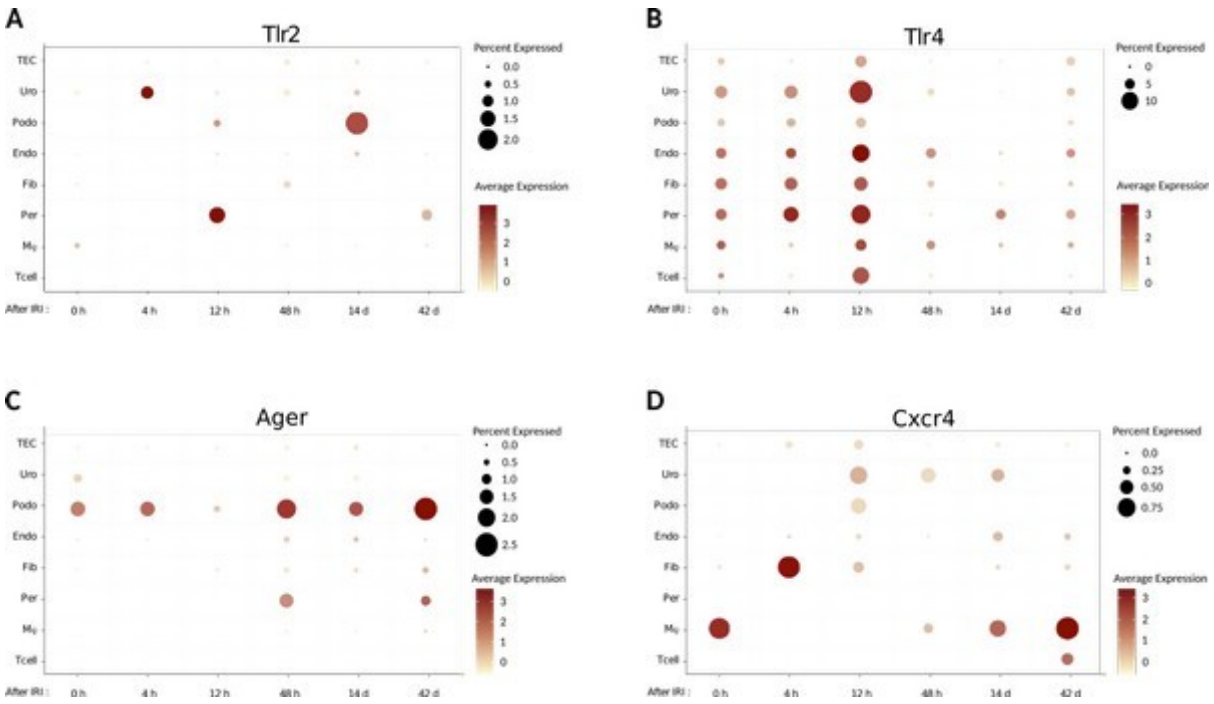

Expression of HMGB1 receptors in murine kidneys after AKI. Dot plot of published snRNA-seq dataset showing **(A)** Tlr2, **(B)** Tlr4, **(C)** Ager, and **(D)** Cxcr4 expression pattern in the proximal tubular cell subtypes along with the time course after bilateral ischemic reperfusion injury (IRI). TEC: Tubular epithelial cells; Uro: Uroepithelial cells; Podo: Podocytes; Endo: Endothelial cells; Fib: Fibroblasts; Per: Pericytes; Mφ: Macrophages; Tcell: T-cells. The diameter of the dot corresponds to the proportion of cells expressing the indicated gene and the density of the dot corresponds to average expression relative to all proximal tubular cells in the whole dataset.

Supplementary figure 2

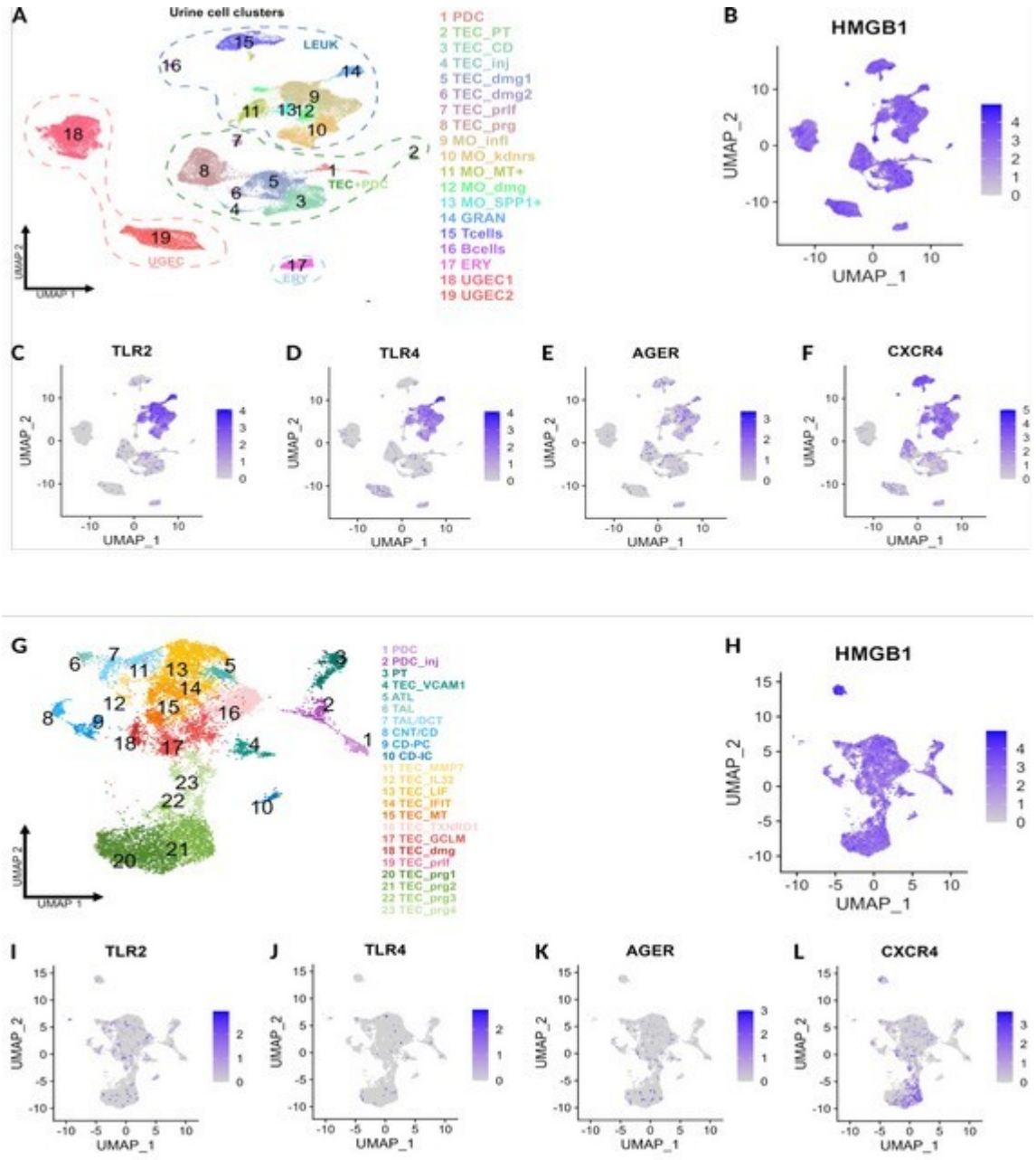

Expression of HMGB1 and its receptors in urine derived human cells. Uniform manifold approximation and projection (UMAP) of 42608 scRNAseq urine transcriptomes from 32 individuals with AKI (Cellular composition is individually diverse but can be broadly grouped into kidney cells (PDC – podocytes, TEC – tubular epithelial cells), urogenital epithelial cells (UGEC) and leukocytes (LEUK) with sporadic contamination of erythrocytes (ERY)) **(A)** and a subsetted UMAP of 12853 urinary renal parenchymal scRNAseq transcriptomes from the same cohort **(G)**. The magnitude of normalized expression of HMGB1 **(B, H)**, TLR2 **(C, I)**, TLR4 **(D, J)**, AGER **(E, K)**, and CXCR4 **(F, L)** is depicted by color code (gray to purple). PT – proximal tubule, ATL – ascending thin limb, TAL – thick ascending limb, DT – distal tubule, CNT – connecting tubule, CD-PC – collecting duct principal cells, CD-IC – collecting duct intercalated cells, MO – monocytes/macrophages, GRAN – granulocytes, inj – injured, dmg –

damaged, prlf – proliferating, prg – progenitor-like, infl – inflammatory, kdnrs – kidney resident.

Supplementary figure 3

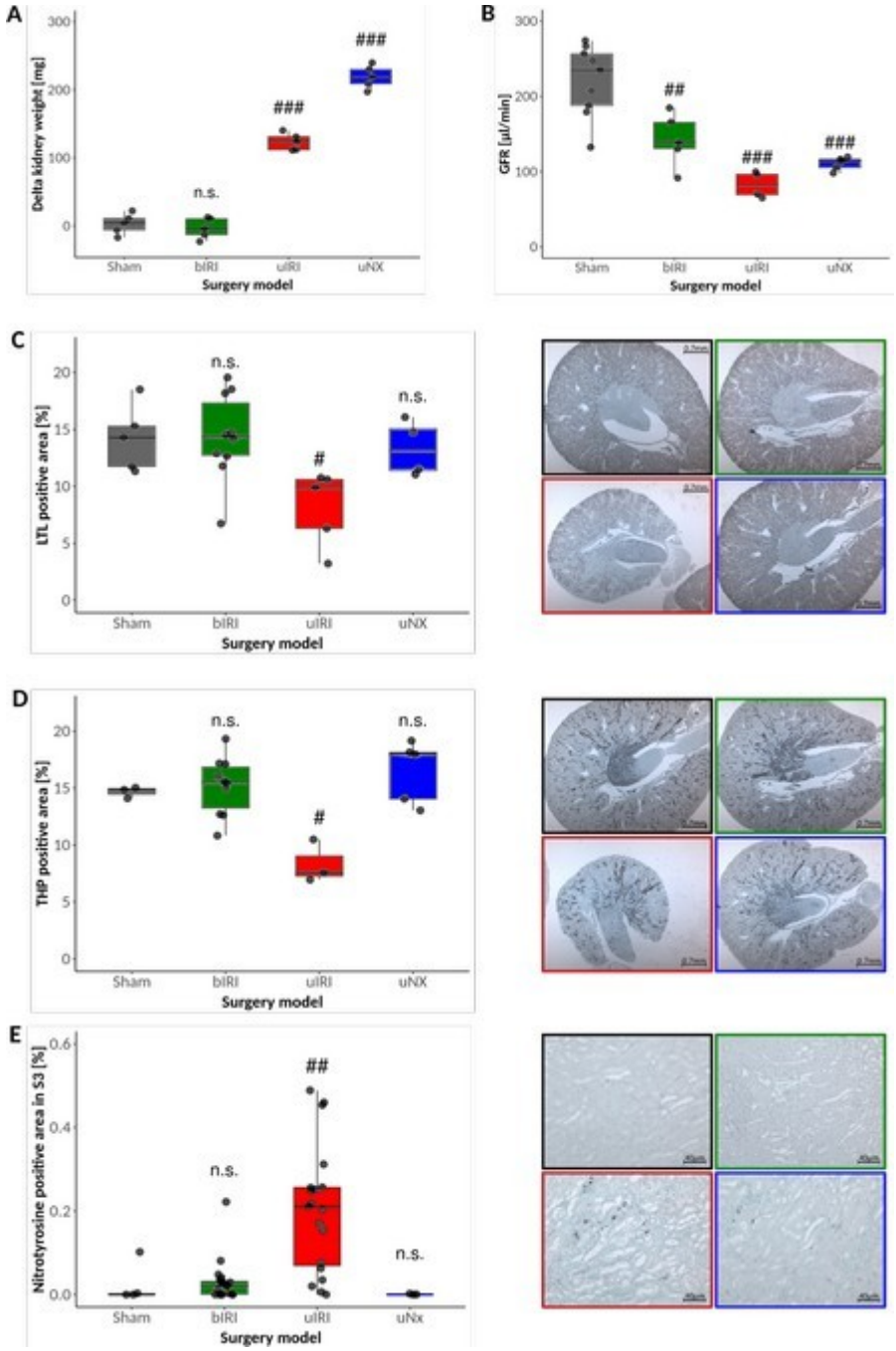

Ischemic necroinflammation followed by persistent hypoxia leads to kidney atrophy. C57BL/6N mice underwent either sham surgery, 20 min of bilateral IRI (bIRI), 40 min of unilateral IRI (uIRI), or uninephrectomy (uNX). The latter was used as a control to assess the effect of compensatory hypertrophy of the residual kidney on GFR. All data were collected at day 30 after surgery. **(A)** Delta kidney weight [mg] as an indicator of renal atrophy and compensatory hypertrophy of the contralateral kidney in response to the surgery model. **(B)** GFR [µl/min] for the same conditions as in (A). Semi-quantitative **(C)** proximal and **(D)** distal tubular mass assessment for the same conditions as in (A). (E) Nitrotyrosine positive area in the S3 segment as a marker of hypoxia for the same conditions as in (A). */# $p < 0.05$, **/## $p < 0.01$, ***/### $p < 0.001$. Data presented in this figure are derived from three independent experiments.

Supplementary figure 4

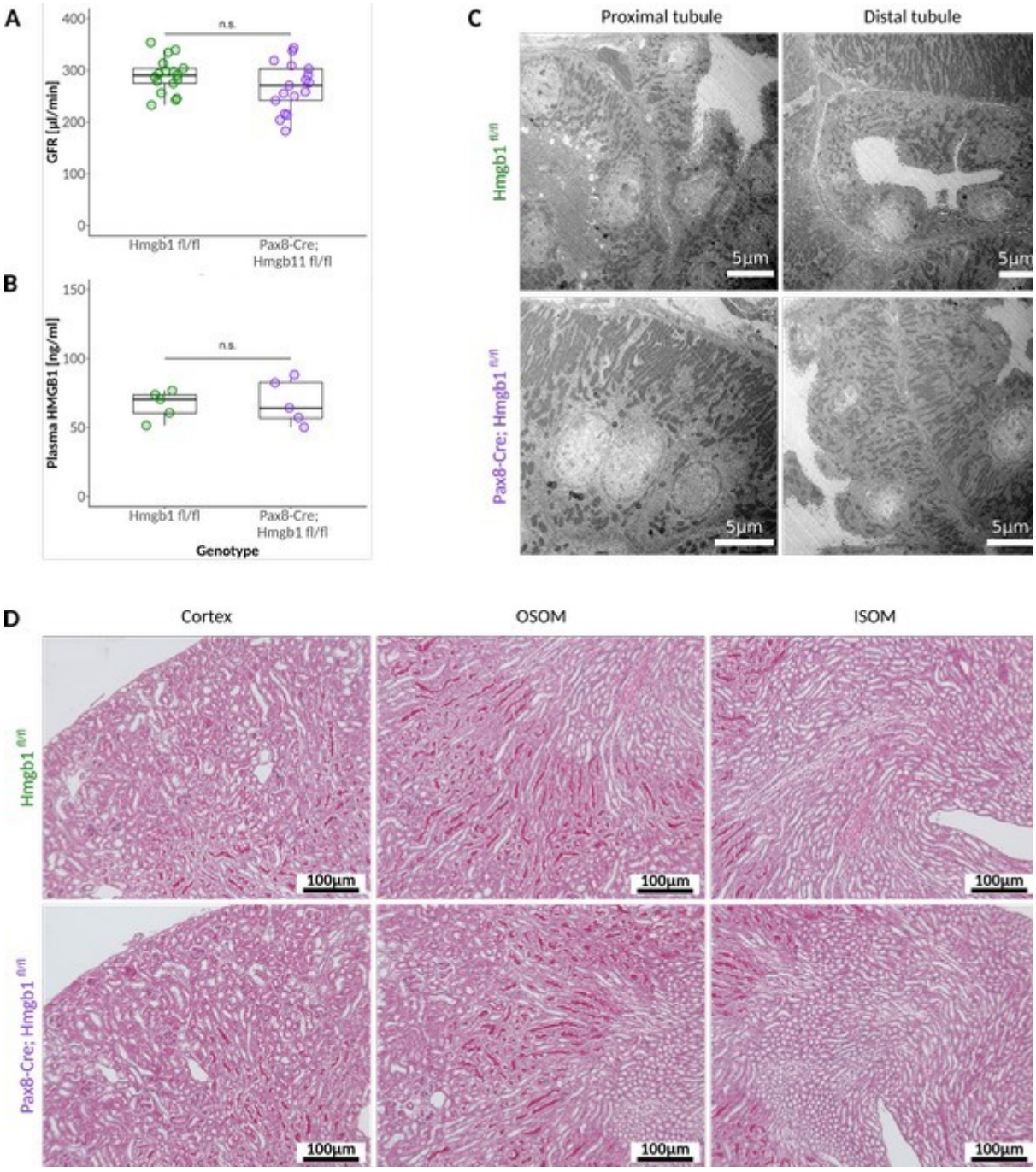

Genetic depletion of Hmgb1 from tubules of adult mice shows no spontaneous phenotype. *Hmgb1*$^{fl/fl}$ and *Pax8-Cre; Hmgb1*$^{fl/fl}$ mice remained unchallenged and underwent **(A)** GFR measurement at 20 weeks of age. **(B)** Plasma HMGB1 levels of both genotypes at day 30 after IRI. **(C)** TEM images **(D)** and representative PAS of both genotypes at 20 weeks of age.

Supplementary figure 5

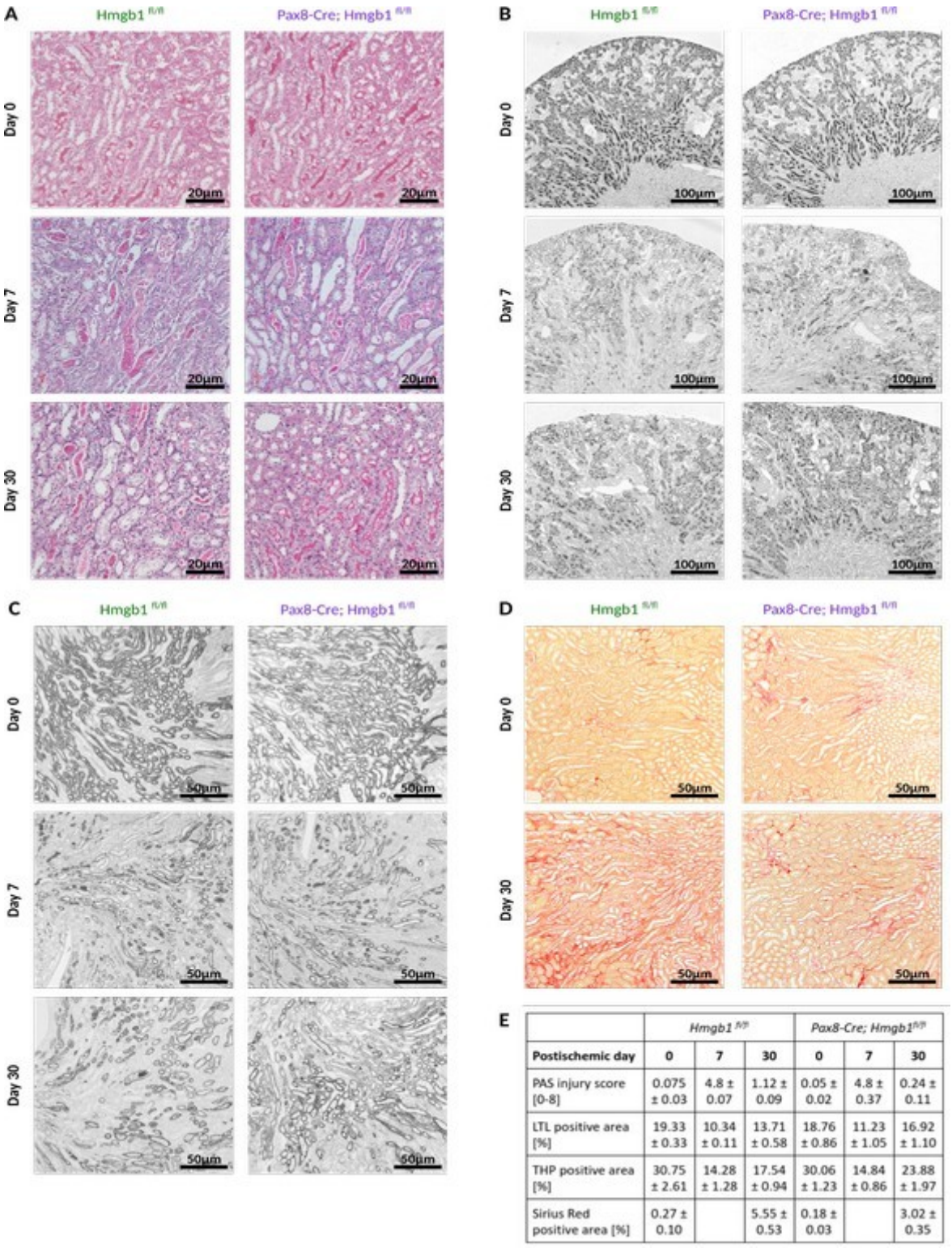

E

	Hmgb1 fl/fl			*Pax8-Cre; Hmgb1fl/fl*		
Postischemic day	**0**	**7**	**30**	**0**	**7**	**30**
PAS injury score [0-8]	0.075 ± 0.03	4.8 ± 0.07	1.12 ± 0.09	0.05 ± 0.02	4.8 ± 0.37	0.24 ± 0.11
LTL positive area [%]	19.33 ± 0.33	10.34 ± 0.11	13.71 ± 0.58	18.76 ± 0.86	11.23 ± 1.05	16.92 ± 1.10
THP positive area [%]	30.75 ± 2.61	14.28 ± 1.28	17.54 ± 0.94	30.06 ± 1.23	14.84 ± 0.86	23.88 ± 1.97
Sirius Red positive area [%]	0.27 ± 0.10		5.55 ± 0.53	0.18 ± 0.03		3.02 ± 0.35

Tubular HMGB1 deficiency does not attenuate ischemic AKI but AKI/CKD transition. Representative images **(A-D)** and quantification **(E)** of kidneys from sham operated (day 0) and postischemic (day 7, day 30) Hmgb1$^{fl/fl}$ and Pax8-Cre; Hmgb1$^{fl/fl}$ mice. **(A)** PAS staining, **(B)** Lotus tetragonolobus lectin staining, **(C)** Tamm-Horsfall-protein staining, and **(D)** Sirius

red staining. **(E)** Values given in each cell are mean ± standard error of the mean (SEM). Data presented in this figure are derived from at least two independent experiments.

Supplementary figure 6

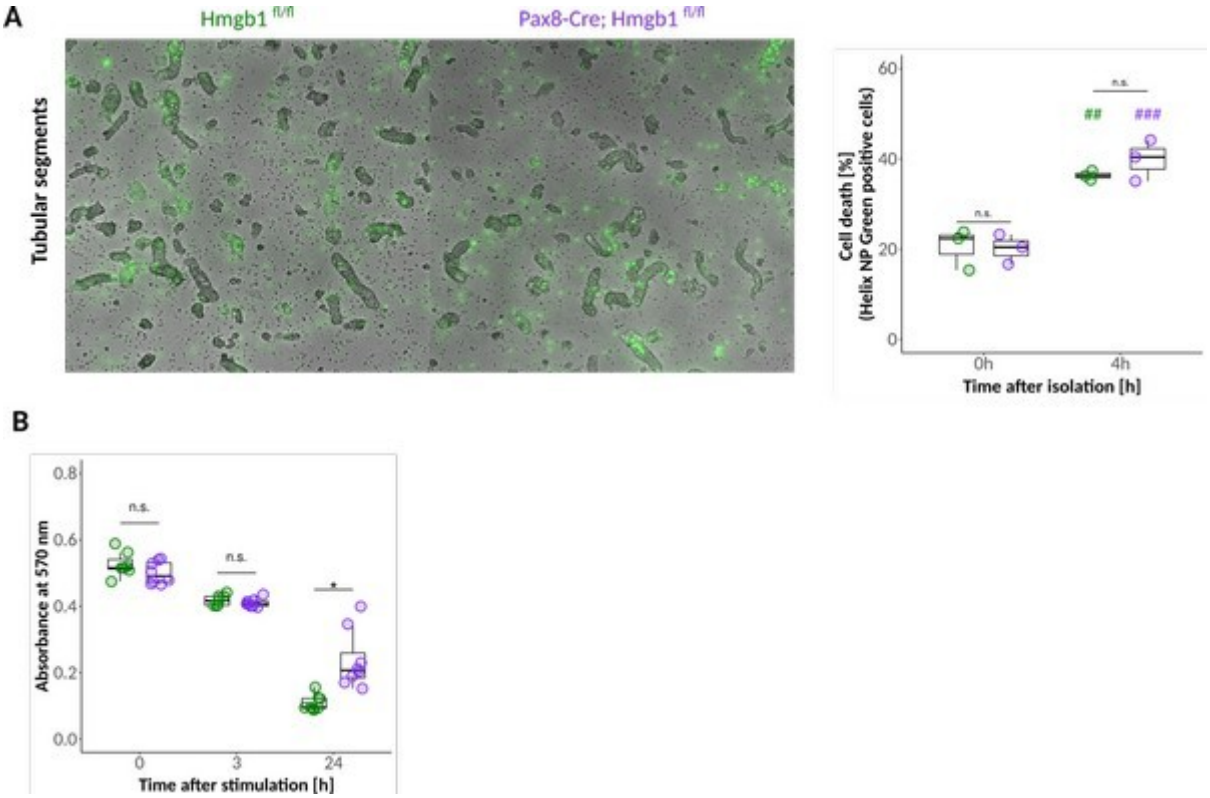

HMGB1 affects the susceptibility of tubular cells to prolonged oxidative stress. **(A)** Helix NP green cell death assay for primary murine TEC isolates at 0 and 4 h after isolation and representative pictures at 4 h in response to genotype. **(B)** Metabolic activity of primary TECs of both genotypes in dependence of time after treatment with 1 mM H_2O_2.

Supplementary figure 7

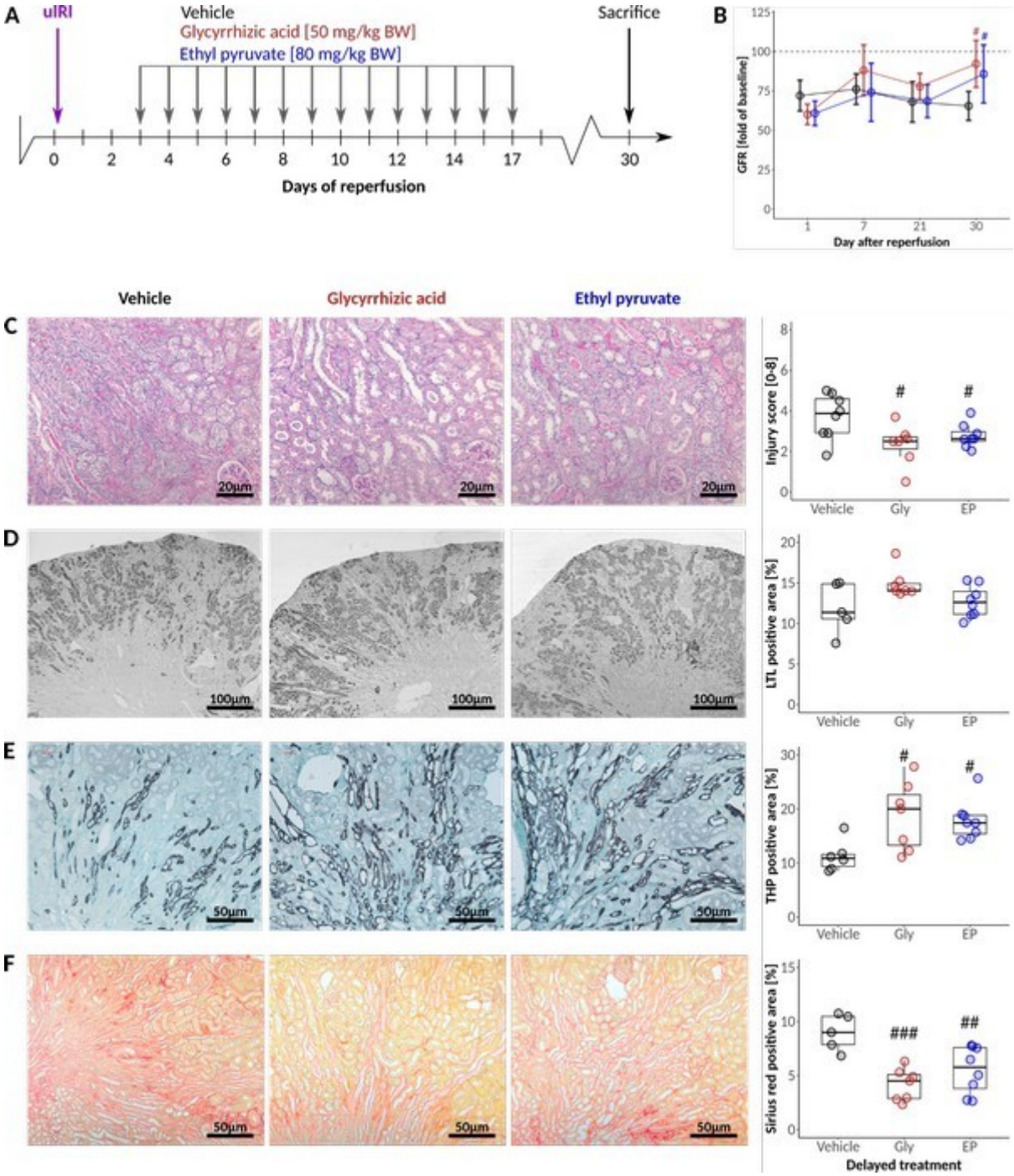

Delayed onset treatment with HMGB1 inhibitors ameliorates post-ischemic phenotypes. **(A)** C57BL6/J mice were challenged with 17 min unilateral IRI and treated with Gly and EP at the indicated time points, with the onset of treatment 72 h after reperfusion. **(B)** Changes in GFR (pre-surgery values for each mouse defined as 100%) after IRI in response to vehicle, Gly and EP treatment. Quantification and representative images for **(C)** semi-quantitative injury scoring based on PAS stainings, **(D)** proximal and **(E)** distal tubular mass assessment, and **(F)** fibrosis staining at 30 days after IRI. */# $p < 0.05$ Data presented in this figure are derived from two independent experiments.

Supplementary video 1

The mp4-file shows time-lapse images of the experiments conducted and presented in supplementary figure 6A.

Supplementary video 2

The mp4-file shows time-lapse images of the experiments conducted and presented in main figure 5A.